

Petrochemical Characteristics of Granitoid Rocks in the Southern part of Maungmagan Area, Launglon Township, Tanintharyi Region

Day Wa Aung, Myat Thuzar Soe, Thanda Sein, Aung Aung Zarni and Su Su Hlaing*
Department of Geology, Yangon University

Abstract

The research area is situated in Launglon Township, Dawei District, Tanintharyi Region, covering about 64 square kilometers. It lies in the Shan Tanintharyi Block, representing the southern part of tin-bearing granitoid belt of Southeast Asia. The area is made up of NNW-SSE trending granitoid rocks; including porphyritic biotite granite, biotite granite, porphyritic biotite microgranite, hornblende biotite granodiorite and aplite. Structurally, two minor fault systems are recognized from the satellite image and field evidences. These are NW-SE and Nearly N-S trending longitudinal fault and NE-SW trending cross fault. Joint pattern shows that there were NE-SW compressional and NW-SE extensional force in the area. Nearly N-S trending aplite dyke is intruded into biotite granite and then aplite dyke contains molybdenite which is an important source of economic interest. Geochemically, the granitoid rocks fall in the granite and monzonite field. They are subalkaline affinity and belong to the calc-alkaline series. Moreover, porphyritic biotite granite, biotite granite and porphyritic biotite microgranite fall in the high potassium calc-alkaline series and hornblende biotite granodiorite falls in the calc-alkaline series, metaluminous to slightly peraluminous in nature, and I type in origin. The decreasing of Al_2O_3 , CaO, P_2O_5 , MgO, Fe_2O_3 , MnO and TiO_2 with increasing SiO_2 suggests that the granitoid rocks were formed due to fractional crystallization during magmatic evolution. According to field evidences and petrographic characteristics, the granitoid rocks in the study area are considered to be magmatic origin. Liquidus temperature can be estimated for porphyritic biotite granite and porphyritic biotite microgranite as $705^\circ C$, biotite granite as $710^\circ C$ and that of hornblende biotite granodiorite is $695^\circ C$. Generally, it may be suggested that the granitoid rocks in the study area may crystallize at depth between 20 km and 22km and the depth of emplacement is estimated at mesozone. Radiometric dating by U-Pb Zircon age method indicates that the age of porphyritic biotite granite is 61 ± 2 Ma, biotite granite is 60.58 ± 0.75 Ma and that of porphyritic biotite microgranite is 59.04 ± 0.53 Ma. Therefore, the granitoid rocks in the study area were successively emplaced during Paleocene. Granites from the study area can be used as decorative stones and dimensional stones. Granites can also be extracted for construction and road materials. The economic interest of the study area is the occurrence of ore mineral especially molybdenite and the economic minerals of rare earth elements.

Keywords: granitoid rocks, calc alkaline, metaluminous to slightly peraluminous, I type, molybdenite mineralization, Paleocene

I. Introduction

Location of the research area

The research area, lying on the southern part of Maungmagan area, is located in Launglon Township, Dawei District, Tanintharyi Region. It is bounded by Latitude $14^\circ 03' 00''$ N- $14^\circ 08' 15''$ N and Longitude $98^\circ 04' 00''$ E to $98^\circ 09' 00''$ E in one inch topographic map number 95J/4. It extends about 8 km from north to south and about 8km from east to west, covering about 64 km^2 . The location map of the research area is shown in Figure (1).

* Su Su Hlaing, Department of Geology, University of Yangon

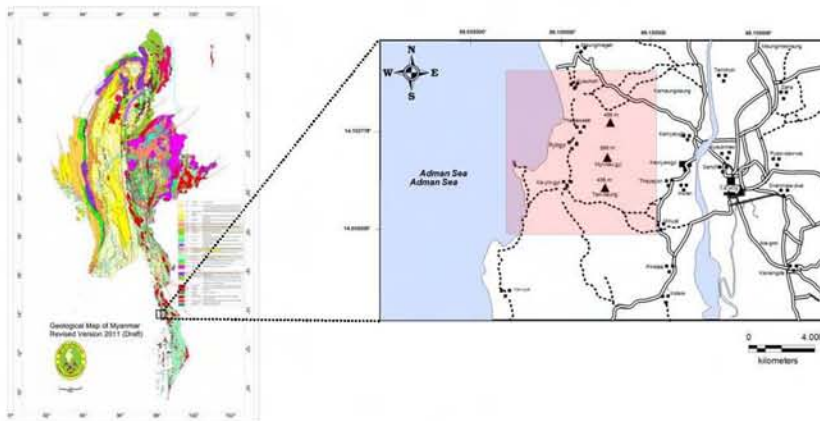


Figure (1) Location map of the research area

Objectives of the research area

The main objectives of the project area are as following:

1. To make a fairly detailed geological map of the area in an appropriate scale
2. To study petrography of igneous rocks of the project area
3. To study the petrochemical characteristic of granitoid rocks exposed in the project area.
4. To mention the economic aspects of the project area

Method of study

The research programme includes the field and laboratory studies. Before the field investigation, various literature and previous works were studied. Geological field works were carried out about one month during the year 2015 to 2016. Firstly, the reconnaissance survey of the project area was made in April, 2016 and then field checking was carried out in July, 2016. Detailed geological studies were made on the basic of the geological map of the previous workers. Lithology, contact boundary and geological structure of the rock units are recorded in the field. The representative samples were collected from each rock unit. Each sample was named base on colour index, mineral composition, texture and natures of their occurrences in the field. The contacts of lithology and structural characteristic were interpreted from the landsat satellite and aerial photographs. About (80) thin sections were prepared for microscopic studies. The detail mineralogical and petrological characteristics of minerals and rocks were studied by using Polarizing microscope. The compositions of plagioclase were determined by using Michel-levy's method. The modal composition of the representative samples were determined by point counting. These data are plotted on the IUGS's classification of igneous rocks diagram of Le Maitre (2001). Major, minor and trace elements of granitoids rocks were determined with XRF analysis. Analysed data are plotted by using GCD kits software and SPSS16 software.

II. Regional Geologic Setting

The research area lies in the southern continuation of the Shan Tanintharyi Block of Maung Thein (1974, 2000) or Sino-Burma Range of Bender (1983). The study area forms a part of the Tanintharyi granite belts, which is actually a part of Western tin-bearing batholiths called Western Tin belt of South East Asia tin provinces of Mitchell (1977), Thein (1983), Nyan Thin (1984) and Cobbing et al (1992). The study area is mainly composed of gneissoid rocks of Coastal Range Granite of Bender (1983). The regional geologic setting of the study area is shown in Figure (2). There are at least six major gneissoid plutons in the Tavoy area, but detailed mapping of the major pluton has yet to be undertaken. The gneissoid plutons intruded into the metasedimentary rocks of the Mergui Group of Brown and Heron (1923), Chhibber (1934) and Pascoe (1959). The gneissoid plutons and batholiths are markedly elongated shape with the longer axes parallel to the NNW-SSE trend of the country rocks (Mergui Group). Tin-tungsten (Sn-W) mineralization is closely related and spatially with gneissoid rocks in this belt. Particularly in the study area, the host rock is sedimentary and meta-sedimentary rocks of Mergui Group were possibly regarded as the Carboniferous-Upper Permian age of Win Swe (2012) according to the stratigraphic correlation and relationship.

The research area is corresponding to a part of the Central gneissoid belt of Khin Zaw (1990). He described that the Central gneissoid belt formed a narrow linear belt of 1450 km long which are dominantly Calc-alkaline and fall in the Peraluminous field, according to petrographic and geochemical data. The gneissoid rocks were possibly emplaced during the continental arc collision at the early stage of westward migrating, east dipping subduction zone during Late Mesozoic to Eocene time. The Central gneissoid belt is developed in the tectonic setting of subduction related magmatic arc, Maung Thein (1986).

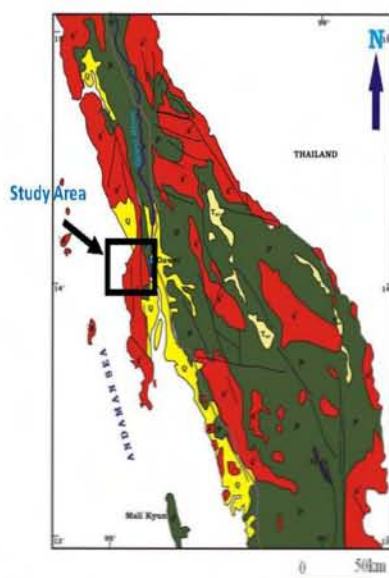


Figure (2) Regional geological map of the study area

(From Geological Map of Myanmar Survey Department, 1977)

III. Petrography

There are three major units exposed in the study area. These are (1) Porphyritic biotite granite unit (2) Porphyritic biotite microgranite unit and (3) Biotite granite unit. Two minor rock types are hornblende biotite granodiorite and aplite. Quartzo-feldspathic veins and

quartz veins are intruding into the older granitoid rocks. The geological map of the study area is shown in Figure (3). The composition of the granitoid rocks plotted on the IUGS classification diagram is shown in Figure (4).

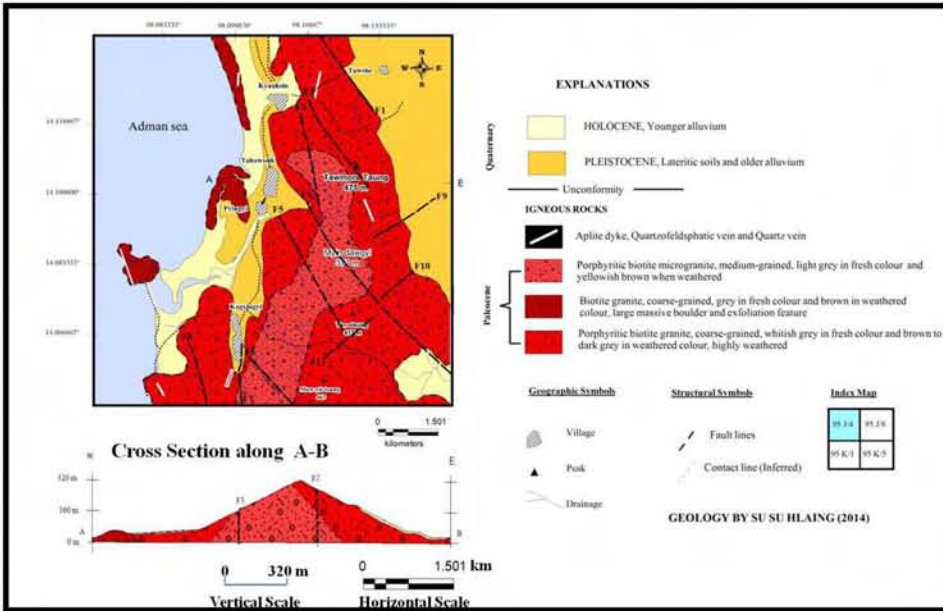


Figure (3) Geological map of the study area

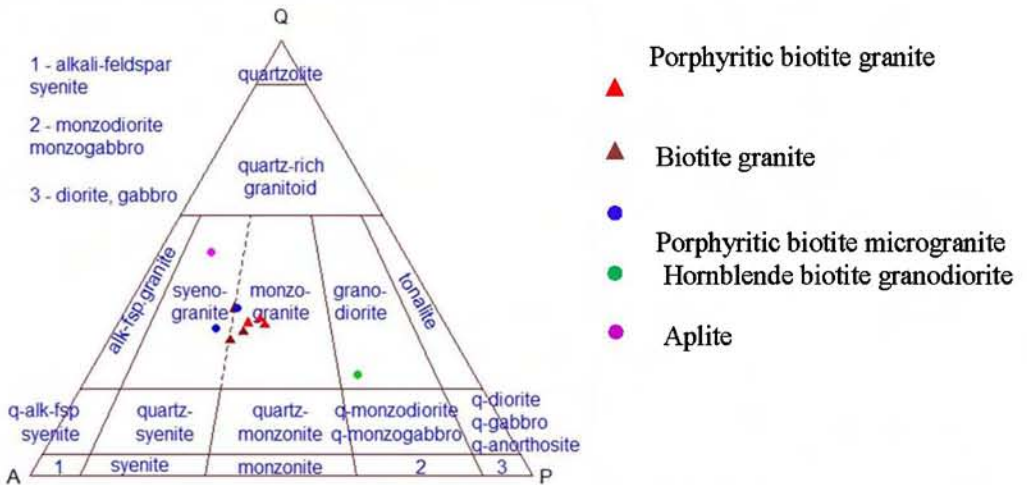


Figure (4) Modal composition of the granitoid rocks plotted on the IUGS classification diagram (Le Maitre, 2001)

Field description of granitoid rocks

Porphyritic biotite granite is the most abundant and well exposed at Tawmore taung, Tan-daung taung, Myindawgyi taung and also at the western flank of the range, Maungmagan village, Kyauksin village, Thabawseik village and Pyingyi village, Figure (5) (A). The phenocrysts (about 2cm to 6cm in length) are exclusively alkali feldspars which are randomly oriented, Figure (5) (B). Brown to dark grey colour on weathered surface

and whitish grey colour on fresh surface. It occur not only large massive boulder but also highly weathered nature. Homblende biotite granodiorite occur as small outcrop within the porphyritic biotite granite unit.

Biotite granite is well exposed at the western costal part of the study area, especially Myawyt, Figure (5) (C, D) and Maungmagan Beach. It is brown on weathered surface and gray colour on fresh surface. Small rounded (or) oval shape xenoliths are abundant in biotite granite.

Porphyritic biotite microgranite is the second major unit in the study area and occurs at the central part and the western flank of the range, Figure (5) (E). Feldspar phenocrysts show parallel alignment at the contact margin and it flow direction is 145° - 325° , Figure (5) (F).

Aplite dykes and veins are intruded into porphyritic biotite granite unit and biotite granite unit. Aplite dyke is 5 m width and 122m long that cuts across biotite granite Figure (5) (G). Molybdenite specks are observed in aplite at Myawyt area. It is trending nearly N-S, (175° – 355°). It shows sugary texture in hand specimen and is characterized by even grain-size that rarely exceeds 2 mm in diameter.

In the study area, small enclaves are most common in biotite granite at beach side. The enclaves in this area are igneous origin of diorite and microdiorite. The contact between enclave and the host rock are sharp. Diorite enclaves are irregular in shape and about 20 cm to 30cm in size, (5) (H). Microdiorite enclaves are smaller in size (about 15 cm to 20 cm in diameter) and exhibit various shapes such as rounded, ellipse and elongated.

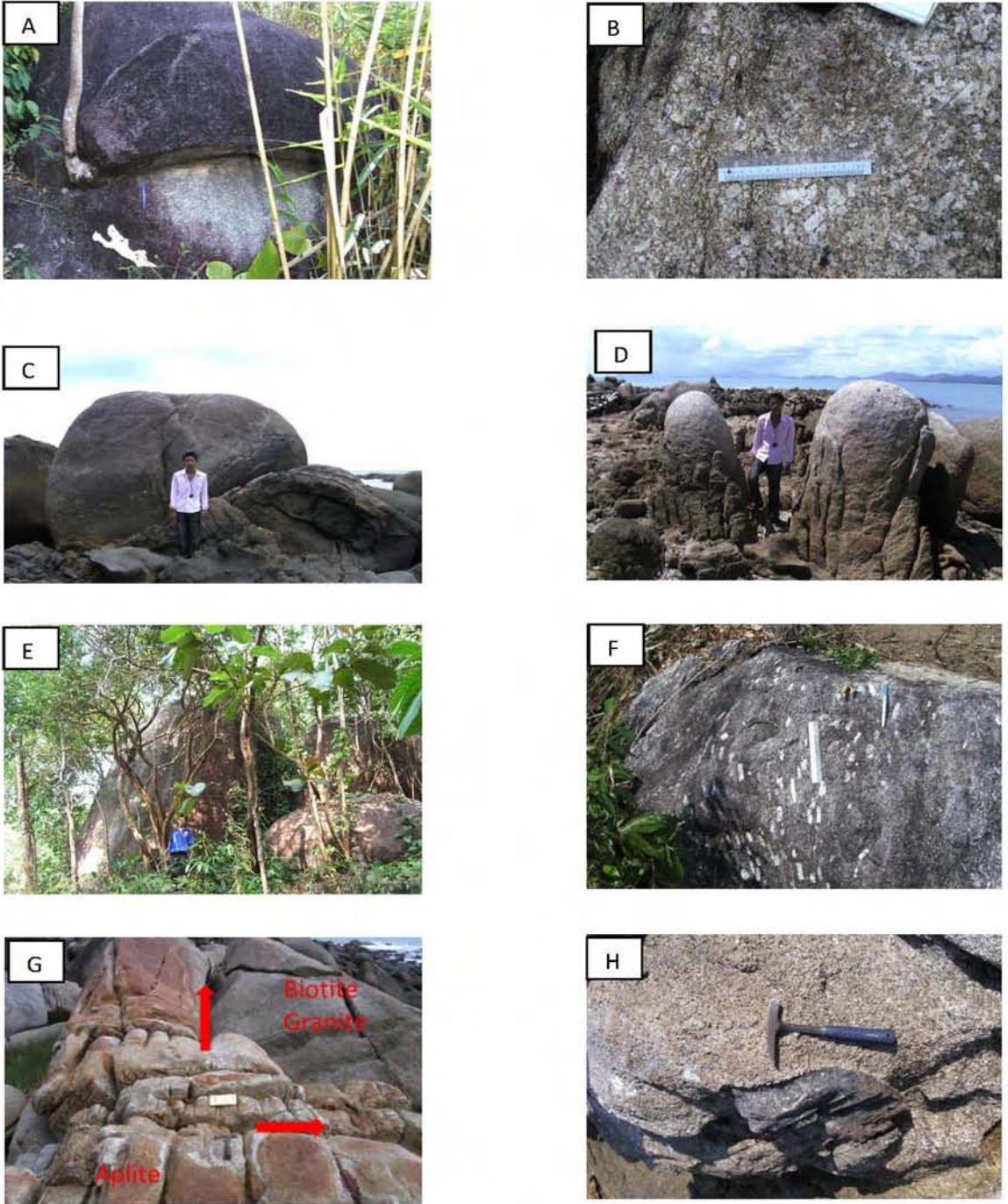


Figure (5) (A) Exposure nature of porphyritic biotite granite
 (B) Close up view of porphyritic biotite granite
 (C) and (D) Outcrop nature of biotite granite
 (E) Boulders of porphyritic biotite microgranite
 (F) Close up view of porphyritic biotite microgranite
 (G) Aplite dyke intruded into biotite granite
 (H) Diorite xenolith in biotite granite

Petrography of granitoid rocks

Porphyritic biotite granite has coarse-grained texture, porphyritic texture and hypidiomorphic granular texture. It is mainly composed of alkali feldspar phenocrysts, quartz, plagioclase and biotite. Zircon, sphene, apatite and magnetite are accessory minerals. Alkali feldspars are represented by perthitic orthoclase and microcline, Figure (6) (A). The size of perthitic orthoclase and microcline are between 4 mm to 6 mm in diameter. Microcline intergrowth with sodic plagioclase forms microcline perthite. Sericitization is well developed in orthoclase and normal zoning is common in plagioclase, Figure (6) (C). The composition range of plagioclase is An_{9-12} . Myrmekitic textures are also seen in boundary of plagioclase, Figure (6) (B). Quartz shows undulose extinction. The aggregates of very small anhedral quartz grains along the margin of large grain found as garland form and it is the characteristic effect of stress. Biotite is observed as subhedral flaky form and some altered to chlorite, Figure (6) (D). Zircon occurs as inclusion in biotite.

Biotite granite is coarse-grained and hypidiomorphic granular texture and mainly composed of alkali feldspar, quartz, plagioclase and biotite. The accessory minerals consist of zircon, Figure (7) (B) sphene, Figure (7) (C) epidote, chlorite, magnetite and muscovite. Quartz is found as anhedral form, large grains and size varies from 2 mm to 6 mm in diameter. Perthitic orthoclase is formed by exsolution of albite rich feldspar and potassium rich feldspar. Flame perthite, stringlet perthite and string perthite are also encountered in biotite granite, Figure (7) (A). Microcline is subhedral and shows cross-hatched twin. The composition of plagioclase is (An_{9-14}) to be albite to oligoclase. Myrmekitic texture is characterized by the minute worm like bodies of quartz enclosed in sodic plagioclase, usually oligoclase. It results from marginal part of potash feldspar especially in contact with plagioclase, owing to late magmatic or post consolidation reaction (After Williams, Turner and Guilbert, 1982). Bulbous myrmekite develop at the margin of the deformed potash feldspar (Phillip, 1974).

Porphyritic biotite microgranite is medium-grained and shows porphyritic, hypidiomorphic granular texture. It is mainly composed of quartz, alkali feldspar and plagioclase. Biotite is minor constituent. The accessory minerals are sphene, zircon and magnetite. Quartz, Orthoclase and plagioclase occur as phenocrysts, Figure (7) (D). Orthoclase shows simple contact twin and string perthite are also noted. Worm-like quartz is present along the plagioclase, given rise the myrmekitic texture. Most of the quartz observed as interstitials and the composition of plagioclase is mainly albite (An_{10-12}) . Corroded quartz is found in alkali feldspar phenocryst. Biotite is small in size 0.5 mm to 2 mm in diameter and altered to chlorite, Figure (7) (E,F).

Hornblende biotite granodiorite is coarse-grained rock and shows hypidiomorphic granular texture. It is mainly composed of plagioclase, alkali feldspar, quartz, biotite and hornblende. It includes apatite, zircon, chlorite and magnetite as accessory minerals. Plagioclase is the most common mineral in this rock. The composition of plagioclase ranges (An_{11-17}) albite to oligoclase. Plagioclase is mostly euhedral and coarser than others. The grain size varies from 1.5-2 mm in width and 3 mm-6 mm in length. Zoned plagioclases are common and some are altered to epidote, Figure (8) (A). Quartz and alkali feldspar are less abundant than plagioclase. Orthoclase shows simple twin with subhedral form and altered to sericite. Microcline occurs as minor amount and shows cross-hatch twinning. Cluster of apatite enclosed in microcline and quartz as inclusions is also noted Figure (8) (B). Quartz occurs as anhedral grains and 1.5 mm to 2 mm in diameter. Biotite is more abundant than hornblende in this rock. It shows strong pleochroism from yellowish to dark brown. Their

size varies from 1 mm to 3 mm in width and 1.5 mm to 2 mm in length. Some biotite altered to chlorite. Hornblende shows euhedral to subhedral, strong pleochroism with yellowish green to dark green, Figure (8) (C, D).

Aplite is medium grained, allotriomorphic granular texture, Figure (8) (E). It is mainly composed of alkali feldspar, quartz, plagioclase and minor amount of biotite and muscovite. Magnetite and sphene are found as accessories.

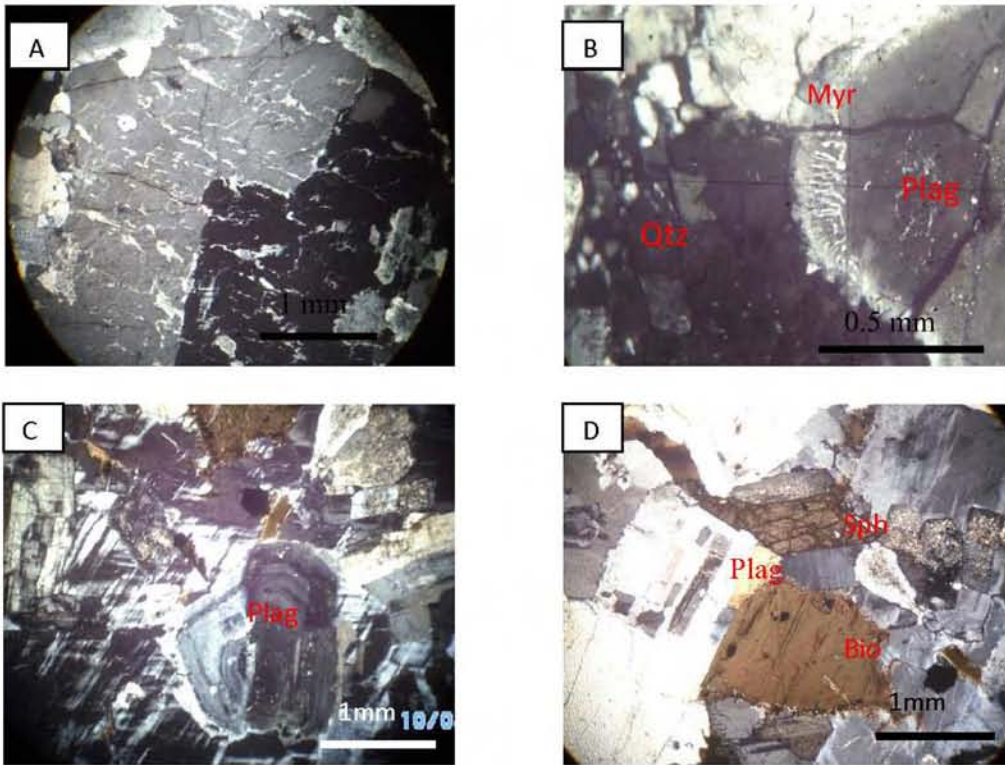


Figure (6) (A) Patch perthite in porphyritic biotite granite (Bet.X.N, 4X)

(B) Rim myrmekite in porphyritic biotite granite (Bet.X.N, 4X)

(C) Zoned plagioclase in porphyritic biotite granite (Bet.X.N, 4X)

(D) Euhedral sphene and subhedral biotite in porphyritic biotite granite (Bet.X.N, 4X)

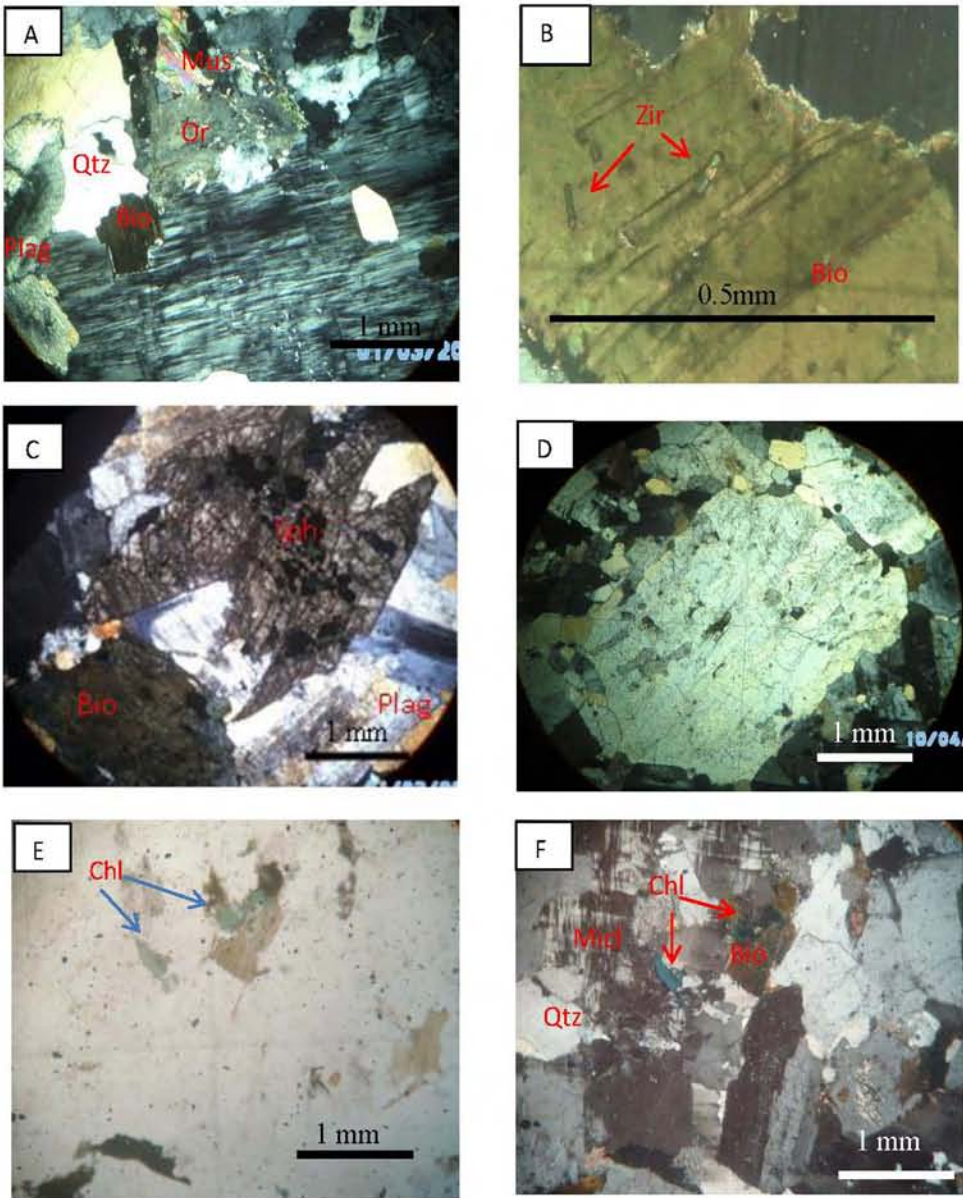


Figure (7) (A) String perthite in biotite granite (Bet.X.N, 4X)
 (B) Zircon inclusions in biotite (Bet.X.N, 10X)
 (C) Subhedral sphene crystals in biotite granite (Bet.X.N, 4X)
 (D) Rim myrmekite in porphyritic biotite granite (Bet.X.N, 4X)
 (E) Zoned plagioclase in porphyritic biotite granite (Bet.X.N, 4X)
 (F) Euhedral sphene and subhedral biotite in porphyritic biotite granite (Bet.X.N, 4X)

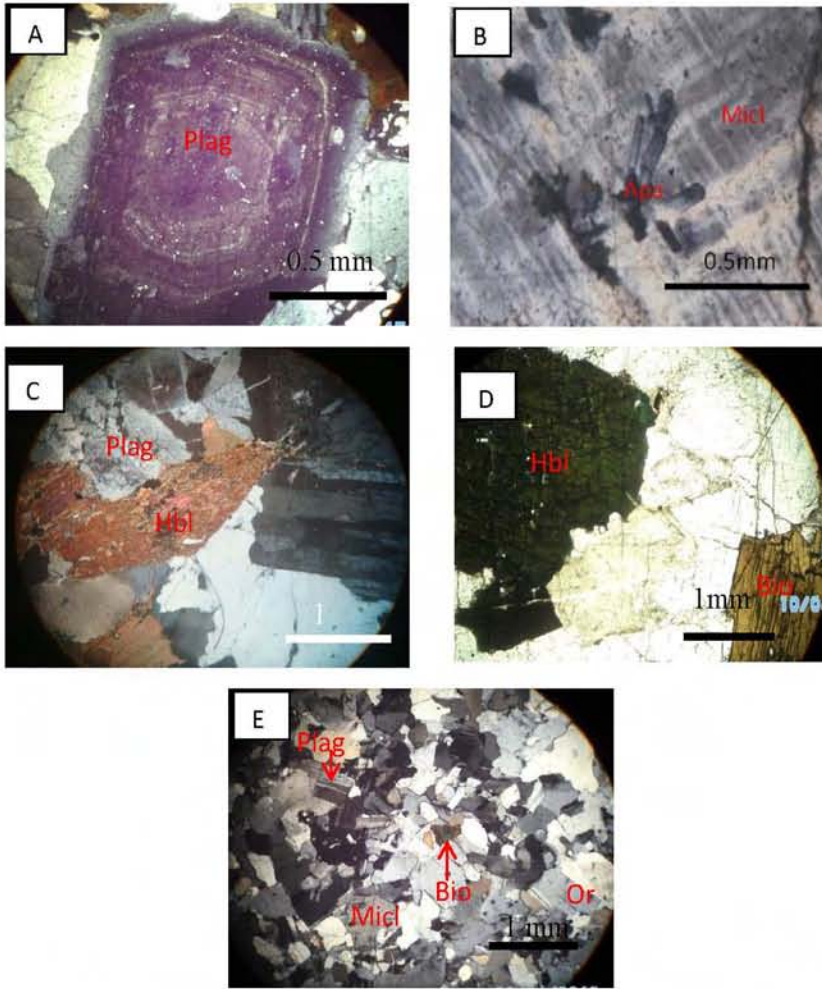


Figure (8) (A) Euhedral, normal zoned plagioclase in hornblende biotite granodiorite (Bet.X.N)
 (B) Cluster of apatite crystals in microcline of hornblende biotite granodiorite (Bet.X.N)
 (C) Euhedral hornblende and plagioclase in hornblende biotite granodiorite (Bet.X.N)
 (D) Subhedral biotite and hornblende in hornblende biotite granodiorite(Under PPL).
 (E) Allotriomorphic granular texture of aplite (Bet.X.N)

IV. Petrochemistry

A total of 25 representative samples (including seven porphyritic biotite granite, six biotite granite, seven porphyritic biotite microgranite, two hornblende biotite granodiorite and three aplite) were selected and analysed from the study area. Major, minor and trace elements of granitoid rocks were determined with XRF analysis.

Presentation for the analytical data

Standard C.I.P.W norm was calculated according to the rule of Hutchison (1975) by using the aid of computer. Differentiative Index or TTDI of Thornton and Tuttle (1960) was calculated from the standard C.I.P.W norms and used as an indicator of bulk composition. These major oxides and trace elements data were illustrated in variation diagram, binary diagrams and ternary diagrams which were drawn by using GCD kit3.0 software, SPSS.16 software and PetroGrap2Beta software.

Geochemical characteristics of granitoid rocks

The granitoid rocks in the study area are porphyritic biotite granite, biotite granite, porphyritic biotite microgranite, hornblende biotite granodiorite and aplite. The SiO₂ content of porphyritic biotite granite ranges from 70.9% to 76.5%, biotite granite (68.2%-71%), porphyritic biotite microgranite (70.2%-73.3%), hornblende biotite granodiorite (60.3%-60.8%) and aplite (76.2%-77.1%). Differentiation index (D.I) of the granitoid rocks in the study area varies from 82.39 to 90.63 in porphyritic biotite granite, biotite granite (79.02-82.29), porphyritic biotite microgranite (82.77-86.98), hornblende biotite granodiorite (65.52-65.69) and aplite (96-96.56).

Standard C.I.P.W normative corundum ranges from 0% to 1.08% with an average of 0.5%. Almost all the rocks are less than 1% normative corundum. Total alkali content (Na₂O+K₂O) ranges from 6.97% to 9.17% with an average of 7.8%. A/CNK = molar Al₂O₃ / (CaO+Na₂O+K₂O) of the granitoid rocks is <1.1. Na₂O content ranges from 3.12% to 5.84% with an average of 3.42%.

In general, XRF geochemical analysis indicates SiO₂ (60.8%-76.5%), TiO₂ (0.182%-0.48%), Al₂O₃ (13.2%-15.5%), Fe₂O₃ as total iron (1.46%-3.69%), MnO (0.04%-0.09%), MgO (0.28%-1.18%), CaO (1.51%-2.98%), Na₂O (3.12%-3.65%), K₂O (3.61%-4.66%) and P₂O₅ (0.042%-0.12%). The bulk rock concentrations of the granitoids are characterized by high SiO₂ and low MnO.

Chemical classification of igneous in the TAS diagram after Cox et al. (1979) is shown in Figure (9) which indicating four groups of igneous rocks and the dividing line between alkaline and subalkaline magma series which is chosen from Miyashiro (1978). The granitoid rocks from the study area are generally range from acid to intermediate group composition and belong to subalkaline affinity. Porphyritic biotite granite, biotite granite, porphyritic biotite microgranite fall in the granite field and hornblende biotite granodiorite falls in the monzonite field.

AFM diagram from Irvine and Baragar (1971) indicating A = (Na₂O+K₂O), F = Fe₂O₃ (as total iron), M = MgO is shown in Figure (10) which subdividing the subalkaline magma series to tholeiitic and calc-alkaline series. This diagram shows that all samples fall in the calc-alkaline series. All samples are of subalkaline affinity and belong to the calc-alkaline series.

Na₂O-K₂O-CaO diagram of Figure (11) indicates that the decrease of CaO with enrichment of Na₂O during the initial stage of differentiation. There is an increase of K₂O with depletion of Na₂O in the later stage of magmatic evolution or magmatic differentiation.

Peraluminous and metaluminous granitoids are chemically defined on the aluminium saturation index (ASI = molar Al₂O₃ / [CaO+Na₂O+K₂O]). It is the chemical discrimination between peraluminous granitoids (ASI > 1) and metaluminous granitoid (ASI < 1) after Zen (1988). In the A/CNK (molar Al₂O₃ / (CaO+Na₂O+K₂O)) Vs A/NK (molar Al₂O₃ / (Na₂O+K₂O)) diagram after Shand (1943), Figure (12), the majority of all samples have 0.98 to 1.07 and plot within the metaluminous to slightly peraluminous field.

Harker's Major oxide variation diagrams are illustrated in Figure (15). The variation diagram of major oxides and SiO₂ are used to interpret the behavior of element in the igneous fractionation. According to Harker's major oxide variation diagram, Al₂O₃, TiO₂, Fe₂O₃ (as total iron), CaO, Na₂O, MgO, MnO and P₂O₅ abundances decrease with increasing SiO₂, showing negative correlation whereas K₂O has positive correlation with SiO₂. It suggests that the granitoid rocks are likely the result of fractional crystallization during magmatic evolution. Generally, major oxide variation diagrams show regular or linear alignment.

In the primitive mantle (Sun & McDonough, 1989) normalize trace element spider diagram of the Figure (13), the granitoids are characterized by strong depletion of Ba, Nb, P and Ti and enrichment of Cs, Rb, U, Th, K, Pb, Nd, Zr and Sm.

The chondrite normalized REEs distribution pattern is shown in Figure (14). REEs chondrite normalized diagram shows bird wing pattern with slightly negative Eu anomaly, ($Eu/Eu^* = 0.39-0.79$). Negative Eu anomaly is normally described to fractionation of plagioclase. The average normalized $(La/Yb)_N = 6.57$ indicating more enrichment of LREE compared with HREE (Rollinson, 1993). The ratio of $(La/Sm)_N = 2.09 - 4.96$ and $(Tb/Yb)_N = 0.75-1.29$ indicates higher concentration of LREE than HREE.

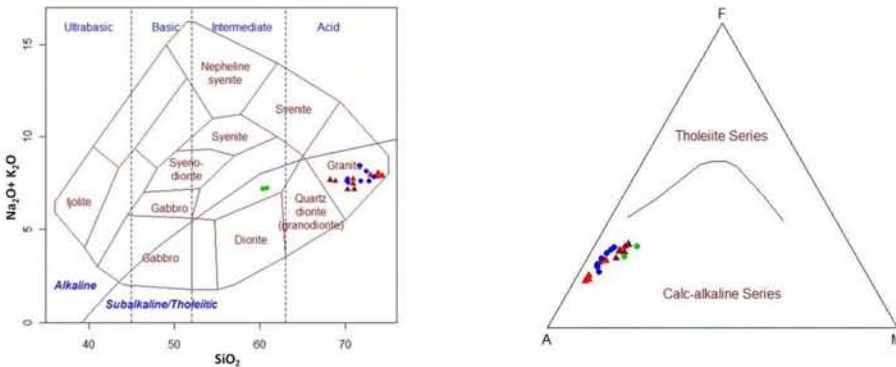


Figure (9) Total Alkali Vs Silica (TAS) diagram after Cox et.al (1979)

Figure (10) AFM diagram after Irvine and Baragar (1971).

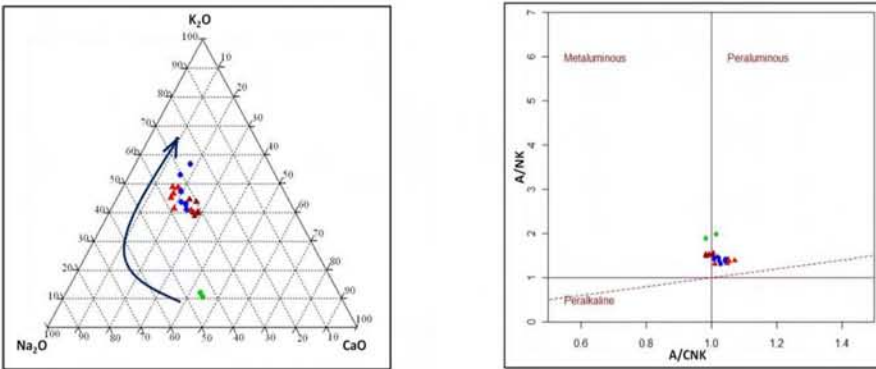


Figure (11) K₂O-Na₂O-CaO ternary diagram

Figure (12) A/CNK Vs A/NK diagram after Shand (1943).

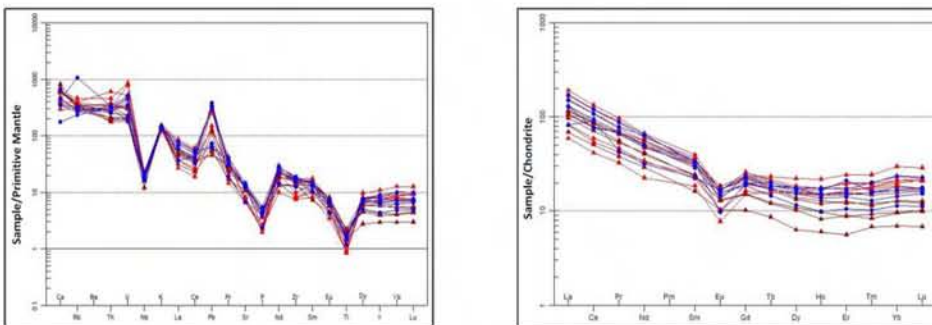


Figure (13) Primitive-mantle normalized trace element multi- variation diagram of normalization values are from Sun and McDonough (1989).

Figure (14) Chondrite-normalized REE pattern of normalization values are from Boynton (1984).

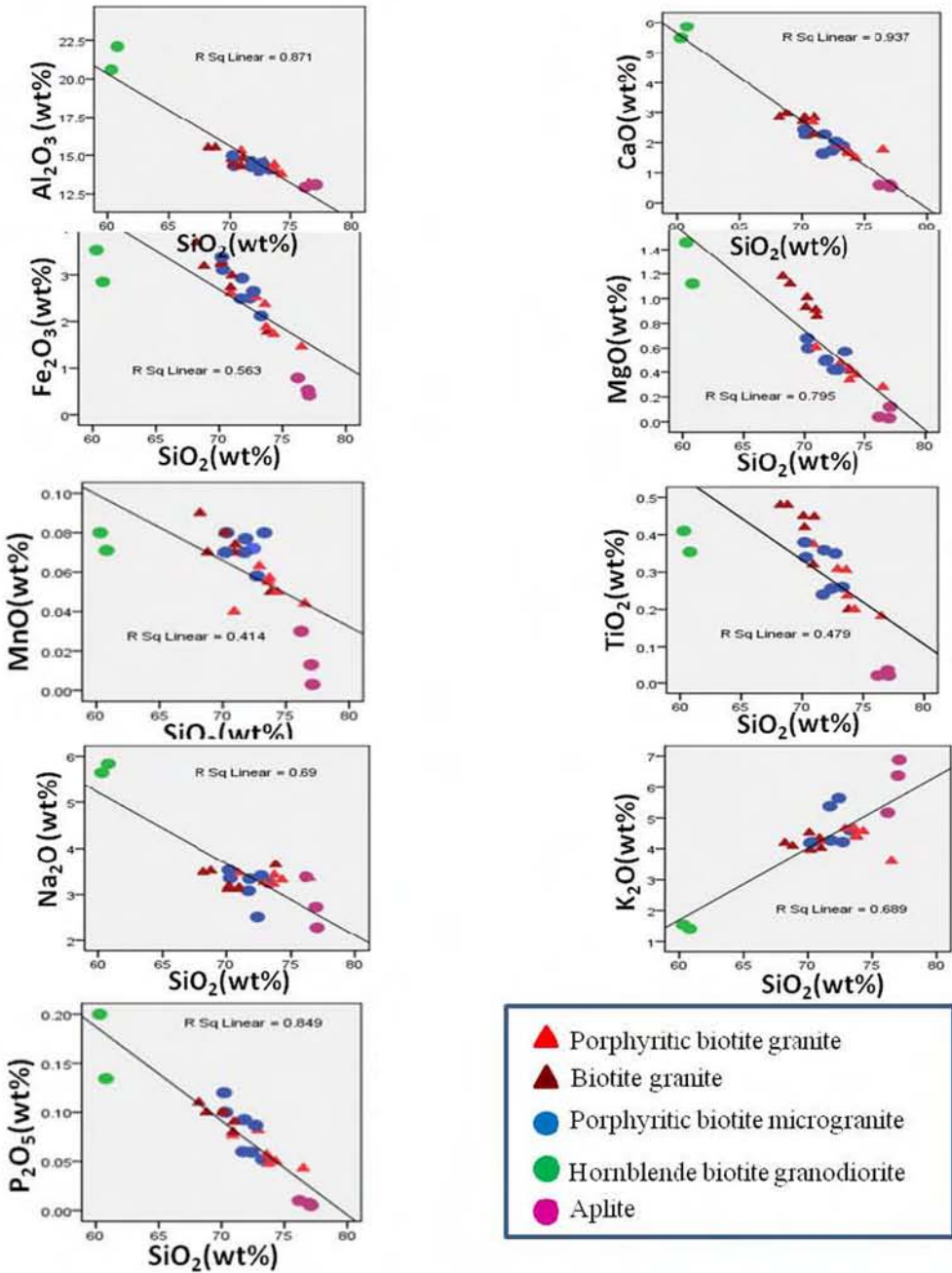


Figure (15) Harker's major oxides variation diagrams showing the correlation between SiO_2 and major oxides of granitoid rocks

Genetic type of granitoid rocks

Major elements characteristic of the granitoid rocks have been used as a key for interpretation of the origin of granite. The linear or regular nature of major oxides and SiO_2 variation diagrams indicate I type character according to Chappell and White (1974). The molecular A/CNK Vs A/NK diagram of Figure (16) shows the discrimination field for different type of granitoids according to Chappell and White (1974). They defined A/CNK

>1.1 as S type and $A/CNK < 1.1$ as I type. The majority of the granitoid rocks in the study area fall in I type granite.

According to field observations, petrographic features, chemical characteristics and economic aspects of granite in the study area, the occurrences of hornblende bearing xenoliths (enclaves), biotite \pm hornblende + sphene + magnetite association, the molecular $Al_2O_3 / (CaO + Na_2O + K_2O)$ ratio of granite range from 0.98 to 1.07 (< 1.1), normative corundum of granite range from 0% to 1.08% with an average of 0.5% ($< 1\%$), linear nature of variation diagrams and associated with molybdenite mineralization; hence the majority of granitoid rocks from the study area are of doubtlessly I type character according to Chappell and White (1974).

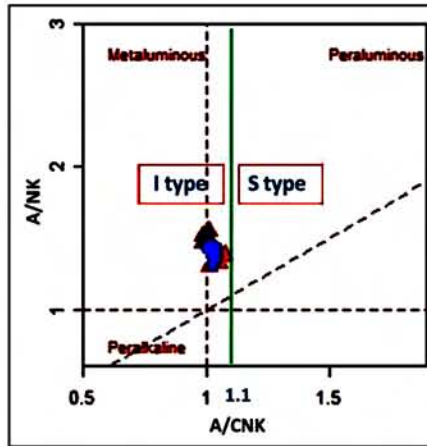


Figure (16) A/CNK Vs A/NK diagram after Chappell and White (1974).

Condition during crystallization of granitoid rocks

Ternary plot of the normative weight percent composition of Quartz- Anorthite-Orthoclase after Tuttle and Bowen (1958) of Figure (17) shows that the majority of all samples lie between the ternary minimum 0.5 kb and 5kb. It can be suggested that the granitoid rocks from the study area were consolidated under lower pressure condition.

Normative Quartz-Albite-Orthoclase ternary diagram after Tuttle and Bowen (1958) of Figure (18) shows H_2O saturated liquidus field boundaries in the system for various water pressures. This diagram indicates that the granitoid rocks from the study area have water pressure within 2kb and 10 kb during crystallization.

If the granitoid rocks were assumed as crystallization at minimum of 2 kb water pressure, their liquidus temperature can be estimated from the differentiation index in 2 kb water pressure diagram, Figure (19). According to this diagram, the liquidus temperature can be estimated for porphyritic biotite granite, porphyritic biotite microgranite at $705^\circ C$ and biotite granite at $710^\circ C$ and that of hornblende biotite granodiorite is $695^\circ C$. Assuming that they were emplaced at P_{H_2O} of 10kb, the temperature of crystallization of the granitoid rocks could be lower.

Depth of the crystallization of the granitoid rocks can be assumed from the depth-temperature relation diagram, after Marmo (1956) is shown in Figure (20). Generally, it may be suggested that the granitoid rocks in the study area may crystallize at depth between 20 km and 22 km. Porphyritic biotite granite and porphyritic biotite microgranite probably may crystallize at 21 km, biotite granite may be at 22 km and hornblende biotite granodiorite may be probably fractionated at 20 km in depth.

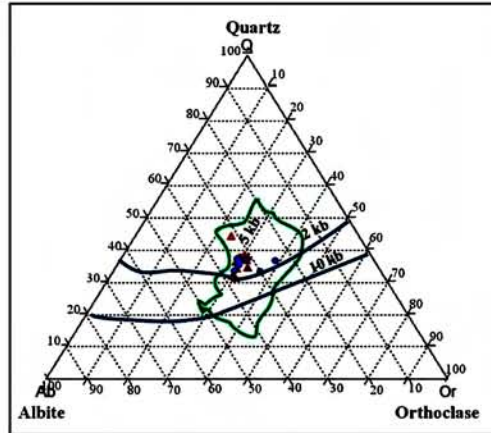
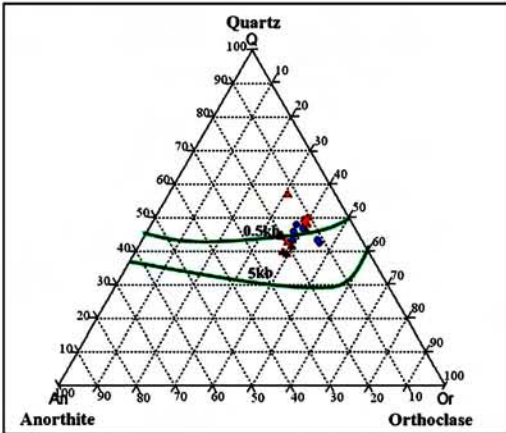


Figure (17) Pressure condition after Tuttle and Bowen (1958)

Figure (18) H₂O saturated liquidus field boundaries in the system for various water pressures after Tuttle and Bowen (1958)

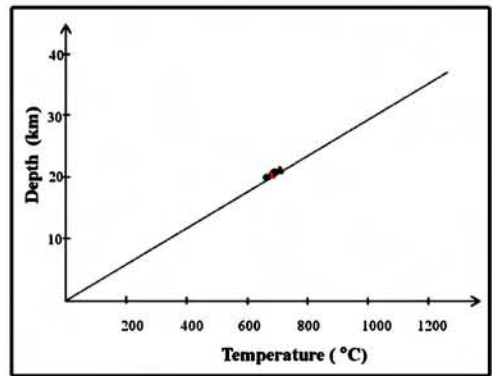
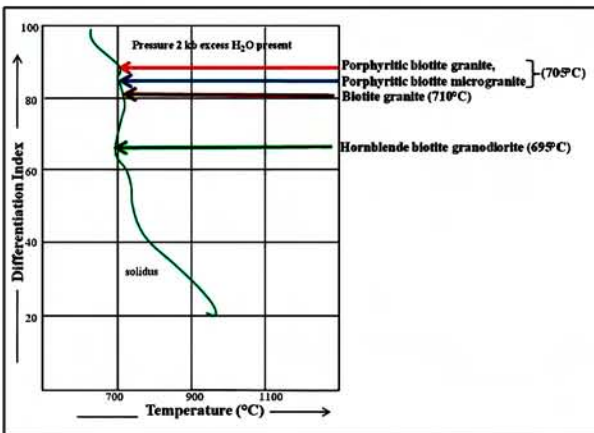


Figure (19) Temperature-differentiation index relation diagram at 2kb water pressure after Piwinski and Wyllie (1970).

Figure (20) Schematic depth-temperature relation diagram after Marmo (1956)

Sequence and age of granitoid rocks

The possible sequence of the granitoid rocks are arranged on the basis of present radiometric dating by Zircon U-Pb method for the representative igneous rocks. The following age of the granitoid rocks were obtained.

- 3. Porphyritic biotite microgranite (59.04 ± 0.53 Ma)
 - 2. Biotite granite (60.58 ± 0.75 Ma)
 - 1. Porphyritic biotite granite (61 ± 2 Ma)
- } Paleocene

V. Economic Aspects of Research Area

Ore mineral occurrence

Only Molybdenite, Figure (21) (A, B) is encountered as an economic mineral in the study area. It found as disseminated grains in aplite dyke. Molybdenite is the chief ore of molybdenum. It can be distinguished by its low hardness, perfect cleavage, streak and tenacity. It is associated with pyrite, Figure (21) (C, D).

Under reflected light, it is extremely reflectance and strong pleochroic, Figure (21) (E). The colour remains white with a pink shade which is more distinct under PPL. The pink shade is highly characteristic in molybdenite. It is consistently developed lamellar (twisted) texture with a perfect cleavage, Figure (21) (F).

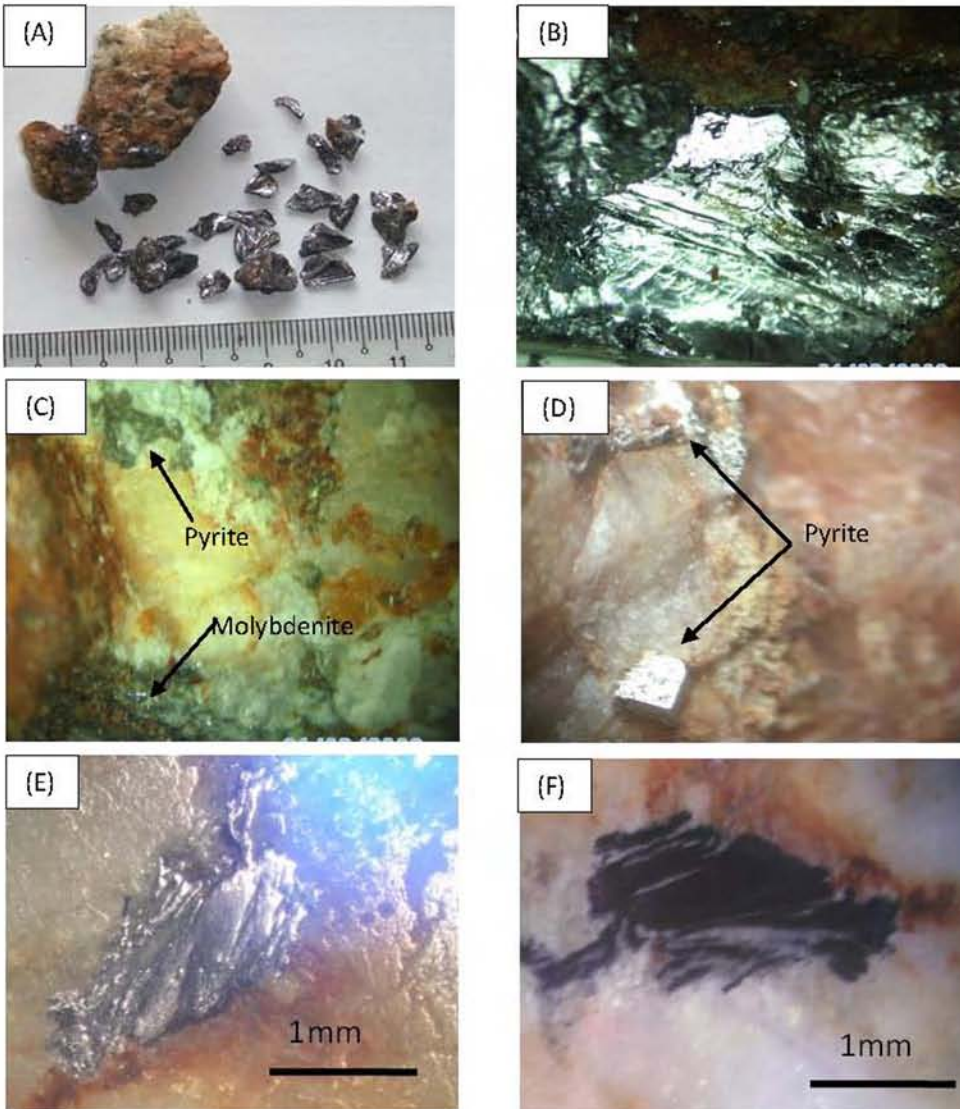


Figure (21) (A) Loose molybdenites
 (B) Close up view of Molybdenite (20X),
 (C) Molybdenite associated with pyrite (10X)
 (D) Close up view of pyrite (40X),
 (E) Highly reflectance nature on reflected light (Under PPL, 4X),
 (F) Lamellar texture of molybdenite on reflected light (Bet.X.N, 4X).

Rare Earth Elements (R E Es)

Rare earth elements are dispersed and not found as concentrated and economically exploitable form. The R E Es are used in many devices that people use every day such as computer memory, DVD's, rechargeable batteries in hybrid vehicles, cell phone, car catalytic converter, magnets, laptop computer, optical quality glass, air pollution control, illuminated screen on electronic device and polishing compound. Therefore, R E Es demand was expected to increase with increase use in portable equipments. The demand for R E Es is rising rapidly but their occurrence in mineable deposit is very limited.

The most abundant rare earth elements are Cerium, Lathanum, Neodymium, and Yttrium. The Cerium content ranges from 33.5 ppm to 107.5 ppm with an average of 67.1 ppm. Lathanum has a range of 8.4 ppm to 59.3 ppm with an average of 34.83 ppm. The Neodymium content ranges from 9.4 ppm to 40 ppm with an average of 20.95 ppm. The Yttrium contents have a range from 17.6 ppm to 49.3 ppm with an average of 30.13 ppm. The highest values are encountered in highly weathered porphyritic biotite granite. These values are higher than average crustal abundances of rare earth elements of Wedephol (1995). Except these, the other rare earth elements are concentrated less than 10 ppm.

Moreover, the average crustal abundances of rare earth elements range from around 150 ppm to 220 ppm. That exceed of many others are mined on an industrial scale, Keith et al (2010). The total R E Es concentrations of granite from the study area divided two groups; 108.77-209 ppm (normal R E Es concentration) and 233-288 ppm (higher R E Es concentration). The higher total R E Es concentrations are encountered from pophyritic biotite granite and pophyritic biotite microgranite. Therefore, granites from the study area can be traced for economic important of R E Es and further study will be necessary for determining economic interest of these elements.

VI. Summary and Conclusion

The present study area is located in southern Myanmar. It lies on the Shan-Tanintharyi Block representing the southern part of tin-bearing granitoid belt of Southeast Asia.

Physiographically, the prominent landmark is Tawmore taung (475 m), the highest peak in the northeastern part of the study area. Structurally, two fault sets can be encountered in the study area. Geologically, the study area is mainly composed of the granitoid rocks which is trending NNW-SSE. The major rock types are (1) Porphyritic biotite granite unit (2) Porphyritic biotite microgranite unit and (3) Biotite granite unit. Two minor rock types are hornblende biotite granodiorite and aplite. Quartzo-feldspatic veins and quartz veins are intruding into the older granitoid rocks.

Petrographically, almost all the granitoid rocks are medium to coarse-grained, hypidiomorphic granular texture although aplite displays allotriomorphic granular texture. Porphyritic texture, perthitic texture and myrmekitic texture are also recognized in these rocks. Biotite is very common minerals in these rocks. The plagioclase composition of granites is albite (An_{9-12}) and its composition range from albite to oligoclase (An_{11-17}) in hornblende biotite granodiorite. Alkali feldspar phenocrysts occur in porphyritic biotite granite. Perthitic texture indicates that the feldspars are formed at high temperature that have cooled slowly, result in unmixing as the solvus curve. The precence of microcline

microperthite and perthitic orthoclase suggest that these rocks are of subsolvus type and crystallized at the temperature of less than 700°C.

Geochemically, SiO₂ contents of the granitoid rocks range from 60.8 to 76.5 wt%. It is characterized by relatively high sodium Na₂O normally > 3.2 %, ASI=molar Al₂O₃/(CaO+Na₂O+K₂O) is from 0.98 to 1.07, ASI <1.1 and Normative corundum < 1% CIPW. It is metaluminous to slightly peraluminous I type granite and associated with molybdenite mineralization. On the basis of major elements of Harker's diagrams, the granitoid rocks may come from same magma source. It is also high K, calc-alkaline affinity, strong depletion of Ba, Sr and Nb and enrichment of Rb, K and La which suggest that contribution of typical crustal melt (Chappell & White, 1992). According to 2 kb water pressure diagram, the estimated liquidus temperature for porphyritic biotite granite and porphyritic biotite microgranite as 705°C, biotite granite as 710°C and hornblende biotite granodiorite as 695°C. According to Depth-Temperature relation diagram, after Marmo (1956), it may be suggested that the granitoid rocks in the study area may crystallize at depth between 20 km and 22 km.

On the basis of field evidence and petrographic characteristics, the granitoid rocks in the study area are considered to be magmatic origin. Geochronologically, U-Pb Zircon age of my study area is (59-61Ma) and the granitoid rocks were successively emplaced during Paleocene.

Finally, the present study area point out Molybdenite associated aplite dyke is very interested for economic prospecting. Granites from the study area can be traced for economic important of R E Es.

Acknowledgements

We gratefully acknowledge the receipt of research funding for this research from the Asia Research Centre, Yangon University. The author is deeply grateful to Professor U Hla Kyi (Part-time Professor, Applied Geology Department, Yangon University) and Professor U Thein Win (Pro-Rector, West Yangon University) and Professor Dr. Khin Zaw (Center of Ore Deposit Research, University of Tasmania, Australia) for their valuable advice, suggestions and discussion. We would like to express our special thanks and appreciation to our numerous colleagues, for their technical helps and continued assistance throughout the preparation of this project.

References

- Alling, H. L., 1932. Perthites, *Journal of the Mineralogical Society of America*, Vol.17, No.2, p. 43-65.
- Chappell, B.W., & White, A.J. R., 1974. "Two contrasting granite types". *Pacific Geology*, vol. 8, p. 173-174.
- Chappell, B.W., & White, A.J. R., 2001. "Two contrasting granite types: 25 years later". *Australian Journal of Earth Sciences*, 48, p. 489-499.
- Cobbing, E.J, et al., 1992. *The Granite of the Southeast Asia Tin Belt*. Overseas Memoir 10, British Geological Survey, London, 369 p.
- Cox, K.G., Bell, L.D., & Pankhurst, R.J., 1979. *The interpretation of igneous rocks*. George, Allen and Unwin, London, 464 p.

- Earth Science Research Division**, 1977. Geological Map of the Socialist Republic of Union of Burma (1:1000, 000 scales) with explanatory Brochure.
- Khin Zaw**, 1990. "Geological, Petrological and Geochemical Characteristics of Granitoid Rocks in Burma; with special reference of the associated W-Sn mineralization and their tectonic setting". Jour. SE Asia Earth Sci. vol. 4, p. 293-335.
- Le Maitre, R. W.** 2001, Igneous Rocks; A classification and Glossary of Term. 2nd ed. Recommendation of the International Union of Geological Science Subcommision on the systematic of Igneous Rocks. Cambridge University Press.
- Marmo, V.**, 1956. "On the emplacement of Granites". Am. Jour. Sci. vol. 254.
- Maung Thein**, 2000. "Summary of the geological history of Myanmar". Paper, p -8. (Unpublished).
- Rollinson, H. R.**, 1993. Using Geochemical data: evaluation, presentation, interpretation, Longman Group UK Ltd. P.352.
- Shand, S., J.**, 1947. Eruptive rocks. Their Genesis, Composition, Classification and their relation to ore deposit. 3rd Edition, John Wiley & sons, New York, 488p.
- Sun, S. S., McDonough, W. F.**, 1989. Chemical and isotopic systematics of oceanic basalts. Publication 42, 313-345.
- Williams, H, F. J Turner and C. M. Guilbert**, 1982. Petrography: an Introduction to the study of Rocks in Thin Section. W. H. Freeman Company, New York.
- Wilson, M.**, 1989. Igneous Petrogenesis; A Global Tectonic Approach. Unwin Hyman London. 466p.
- Win Swe**, 2012. Outline geology and Economic mineral occurrences of the Union of Myanmar. Journal of the Myanmar Geosciences Society, Special Publication No.(1), p.120-125.
- Winter. J. D.**, 2013. An introduction to Igneous and Metamorphic Petrology, Prentice Hall, New Jersey, p.697.

